RESEARCH ARTICLE

Deactivation by S-Glutathionylation overrules activation by PRMT1-dependent asymmetrical di-methylation in PFKFB3

Authors
Jeong-Do Kim[1,#], Young-Sun Yim[1], Michal Brylinski[1], M. Raafat El-Maghrabi[2], Yong-Hwan Lee[1,*]

Affiliations
[1]Department of Biological Sciences, Louisiana State University, 202 Life Science Building, Baton Rouge, LA 70803
[2]Department of Physiology and Biophysics, State University of New York at Stony Brook, School of Medicine, Basic Science Tower, T-6, Room168, Stony Brook, NY, 11794-8661.
[#]Present addresses: NuPotential Inc., Louisiana Emerging Technology Center, 340, E. Parker Blvd., Baton Rouge, LA 70803.

[*]To whom correspondence should be addressed:
Yong-Hwan Lee, Department of Biological Sciences, Louisiana State University, 202 Life Science Building, Baton Rouge, LA 70803; yhlee@lsu.edu; Tel. (225) 578-0522; Fax. (225) 578-7258.

The abbreviations used are: PRMT1, protein arginine methyl transferase 1; N-CH3, PRMT1-dependent asymmetrical dimethylation at arginine residues; ROS, reactive oxygen species; S-Gsh, S-glutathionylation; CDK1, cyclin-dependent protein kinase 1; GSH, glutathione; ox- or reGSH, oxidized or reduced glutathione; PFKFB, 6-phosphofructo-2-kinase/fructose-2,6-bisphosphatase; Fru-2,6-P_2, fructose-2,6-bisphosphate; Fru-6-P, fructose-6-phosphate; AMPPCP, beta,gamma-methylene ATP; PKM, muscle type pyruvate kinase; PFK, phosphofructokinase; O-GlcNAc or O-GlcNAcylation, O-linked attachment of N-acetylglucosamine; AdOX, adenosine-2',3'-dialdehyde; PPP, Pentose Phosphate Pathway; GSHee, ethyl ester GSH; Ribul-5-P, ribulose-5-phosphate; Xyl-5-P, xylulose-5-phosphate; G-3-P, glyceraldehydes-3-phosphate.

Abstract

To understand PFKFB3 control by covalent modifications, the structure/function effect of protein arginine methyl transferase 1-dependent asymmetric di-methylations at Arg131 and Arg134 (N-CH3) and its relationship to S-glutathionylation at Cys206 (S-Gsh) was investigated. Distinctly from the report that N-CH3 is for protection of PFKFB3 from the APC/C-Cdh-mediated polyubiquitination and proteolysis, an increase in the activity for Fru-2,6-P_2 production was shown from a molecular simulation and *in-vitro* tests. The simulation suggested that N-CH3 would uncouple the Fru-6-P entry turn (-^{130}TRERRH-) from its coupling to the π-helix (-^{204}DKCDRD-) by disabling the interaction between Arg131/134 and Asp207. The uncoupling consequently is likely to facilitate the Fru-6-P binding by enhancing the conformational flexibility.

Confirming the simulation, N-CH3 was shown to cause a 5-fold increase in the specific activity (k_{cat}/K_m) mostly through a 4-fold decrease in K_ms for Fru-6-P. A similar extent of activation was induced by Asp207→A mutagenesis, which disables the coupling, while the activation by N-CH3 was almost abolished by Arg131→A mutagenesis. More interestingly, PFKFB3 with N-CH3 could be additionally S-glutathionylated at Cys206, when oxidative stress is elevated. When modified by both N-CH3 and S-Gsh, the activity was decreased, as if there was no N-CH3 at all, suggesting that the deactivation completely overrules the activation.

When HeLa cells were treated for the dual modifications of PFKFB3, the overruling deactivation effect of S-Gsh was prevalent, causing decreases in Fru-2,6-P_2 levels and increases in glycolytic flux redirected to the pentose phosphate pathway. As a result, the levels of NADPH and reduced glutathione were markedly elevated, enhancing cell viability under the conditions of elevated oxidative stress. Altogether, it is suggested that the functional effect of S-Gsh, which represents a mechanism for survival under detrimental oxidative stress, dominates over the effect of N-CH3, which has been suggested as a mechanism for growth.

Keywords: PFKFB3; N-methylation, S-glutathionylation, glycolysis, pentose phosphate pathway,

Introduction

Selective overexpression of the inducible form 6-phosphofructo-2-kinase/fructose-2,6-bisphosphatase (PFKFB3) among the four isoforms (PFKFB1-4) is an essential component of the metabolic reprograming of oncogenic cell transformation [1-8]. PFKFB3 has distinctively high activity for production of fructose-2,6-bisphosphate (Fru-2,6-P_2), which is the most potent allosteric activator of phosphofructokinase (PFK), the rate-limiting enzyme of glycolysis [9-15]. It was recently shown that Fru-2,6-P_2 is also an activator of cyclin-dependent protein kinase 1 (CDK1), which promotes the G_1- to S-phase cell cycle transition [5,16-19]. Moreover, it has been revealed that PFKFB3 in the vascular endothelial stalk cells promotes formation of new blood vessels [20,21]. Altogether, PFKFB3 plays crucial roles in the three hallmarks of cancer: vigorous glycolysis, long known as the Warburg effect [1,7,22], rapid cell cycle progressions [5,16,19,23], and new blood vessel sprouting [20,21,24]. Thus, artificial down-regulation of PFKFB3 activity has been suggested as a new paradigm of the fights against cancer [4,25-28].

It has been shown that PFKFB3 is controlled by various posttranslational dynamic covalent modifications. Its catalytic activity for Fru-2,6-P_2 production is increased upon phosphorylation (O-Pho) at Ser461 [29-31] by various protein kinases but decreased upon S-glutathionylation (S-Gsh) at Cys206 [32]. The resulting changes in Fru-2,6-P_2 levels are the causes of changes in glucose metabolism and the rates of cell cycle progression [16-19,23,33,34]. For better understanding of PFKFB3 functions and controls, we have addressed the molecular basis of Fru-2,6-P_2 synthesis by PFKFB3 through crystallographic studies of PFKFB3 in a native state (pdb code '2AXN'), a pseudo-Michaelis complex (PFKFB3•AMPPCP•Fru-6-P, pdb code '2DWP'), and the product complex (PFKFB3•ADP•Fru-2,6-P_2, pdb code '2I1V') [35,36].

Then, we unfolded the roles of PFKFB3 in the fights against oxidative stress by characterizing S-glutathionylation of PFKFB3 and its functional effects inside cells [32]. It was revealed in the structure of S-glutathionylated PFKFB3 (pdb code '4MA4') that Fru-6-P binding to the catalytic pocket is interfered by the glutathione (GSH) moiety attached to Cys206, resulting in a 4-fold decrease in the activity. Increases in cellular oxidative stress caused S-Gsh of PFKFB3 and, as a result, a decrease in cellular Fru-2,6-P_2 levels and glycolysis was induced inside cells. The event was coupled to enhanced redirection of glucose metabolic flux to the Pentose Phosphate Pathway (PPP). Ultimately, reduction of NADP to NADPH and oxidized glutathione (oxGSH) to reduced glutathione (reGSH), which are necessary for neutralization of reactive oxygen species (ROS), was markedly increased. Thus, S-Gsh of PFKFB3 together with S-Gsh of pyruvate kinase was suggested as one of the crucial mechanisms underlying cell survival under the condition of elevated oxidative stress [37-41].

It was recently shown that PFKFB3 is also asymmetrically di-methylated at Arg131 and Arg134 through the protein arginine methyl transferase 1 (PRMT1)-catalyzed reactions and that the level of this methylation (N-CH3) is maintained higher in proliferating cells [42,43]. A decrease in the level of this N-CH3, which can be elicited by onsets of oxidative stress with an unclear mechanism, was shown to cause a biological effect similar to that caused by S-Gsh of PFKFB3. It has been argued that PFKFB3 is protected from the anaphase promoting complex/cyclosome with Cdh1 (APC/C-Cdh1)-dependent polyubiquitination-mediated proteolysis by N-CH3. Decreases in the N-CH3 levels lead to decreases in PFKFB3 protein levels, causing a same biological effect as deactivation of PFKFB3 inside cells. As a consequence, decreases in Fru-2,6-P_2 levels together with decreased flux of glycolysis were induced to cause the concomitant increases in the increased PPP flux accompanied with increased concentration ratios of NADPH/NADP and reGSH/oxGSH, enhancing cell viability under oxidative stress [42,43].

However, we suspected a possibility of a distinct role of N-CH3, because the site, Arg131/134, belongs to the first turn of an α-helix, which is crucial for catalytic Fru-6-P binding and is within 3.7 Å from Cys206, the S-Gsh site. This structural feature suggests that N-CH3 would affect the activity by altering the Fru-6-P binding and that N-CH3 and S-Gsh affect each other. To address the suspicion, we investigated the functional effects of N-CH3 on the PFKFB3 activity at the molecular level, employing molecular dynamics, site-directed mutagenesis, and kinetics. Then, we investigated the molecular relationships between N-CH3 and S-Gsh and the metabolic effect of their interplay at the cellular level, to evaluate the biological significance. The results of the two aimed studies are reported and discussed here.

Experimental procedures:

Materials

The following materials were obtained from the sources indicated: dimethyl sulfoxide, oxidized L-glutathione (oxGSH), reduced L-glutathione (reGSH), and BCNU (Sigma Chemical Co., St. Louis, MO, USA); Qdot 605 ITK streptavidin conjugate kit (2 µM solution), dextran alexafluor 488, anti-V5 antibody, calceinacetoxymethyl ester, PLUS reagent, lipofectamine LTX reagent, and biotinylated glutathione ethyl ester (BioGEE) (Invitrogen Corporation, Carlsbad, CA, USA); anti-glutathione monoclonal antibody (ViroGen Corporation); V5 antibody affinity purified agarose immobilized conjugate (Bethyl Laboratories); goat anti-mouse glutaredoxin-1/GLRX1 antibody (R&D Systems Inc.); and glutaredoxin-1 and glutaredoxin-1 antibody (Abcam).

Plasmid Constructs and Mutagenesis.

Full-length cDNA constructs for human PFKFB3 mutants, Arg131→K, Arg131→A, and Aap207→A, were generated by site-directed mutagenesis using the QuikChange II XL Site-Directed Mutagenesis Kit (Stratagene), following the manufacturer's recommendations and the commercially available vector pcDNA3.1/myc-HisA with human PFKFB3 as a template [32]. The mutants were then subcloned from pcDNA3.1/myc-HisA into the pET3a vector using NheI and BamHI restriction sites to create bacterial expression plasmids. All constructs were sequenced for verification.

Protein Preparation, S-Glutathionylation, N-Methylation, and Western Blotting.

The N-terminal 6XHis-tagged human PFKFB3 and the mutants were expressed in Escherichia coli CL41(DE3) and purified using Ni-NTA affinity columns and, subsequently, Mono Q anion-exchange chromatography. The detailed methods are described elsewhere [36].

To induce protein S-glutathionylation, purified PFKFB isoforms (0.3mg/ml) in a buffer containing 50 mM Tris●HCl (pH 7.5), 10 mM NaP_i, 5% glycerol, and 0.5 mM EDTA were incubated for 30 min with 3 mM of 1:1 molar ratios of GSH to GSSG (total concentration at 3 mM) in 50 mM Tris●HCl pH7.5 at room temperature [32]. For Western blotting, samples were then mixed with Laemmli sample buffer without reducing agent or heating but with 1 mM N-ethylmaleimide (NEM) for the alkylation of accessible thiols on PFKFB3, resolved in non-reducing SDS-PAGE, and transferred to nitrocellulose membranes. The Membranes were probed with anti-glutathione antibody (Virogen), followed by detection with horseradish peroxidase-conjugated secondary antibody (Novagen). Bands were visualized by enhanced chemiluminescence (SuperSignal West Pico, Pierce) according to the manufacturer's instructions. Membranes were subsequently re-probed with anti-PFKFB3 antibody (Abgent).

In vitro PFKFB3 N-CH_3 was carried out using the recombinant human protein arginine methyl transferase 1, which was expressed and purified similarly to the protocol for PFKFB3. PFKFB3 was N-methylated by the recombinant PRMT1 in a buffer containing 50 mM MOPS (pH 7.5), 300 mM NaCl, 2 mM EDTA, 1 mM PMSF, and 0.4 mM S-adenosyl methionine (SAM). For Western blotting, samples were then resolved in non-reducing SDS-PAGE and transferred to nitrocellulose membranes. To detect N-CH_3, the membranes were probed with anti-asymmetric dimethyl arginine antibody (ASYM25, Millipore-Sigma) followed with horseradish peroxidase-conjugated secondary antibody (Novagen).

Measurement of PFKFB3 activity.

The catalytic activity of PFKFB3 for Fru-2,6-P_2 synthesis was performed as described previously [35,44]. The 2-Kinase reactions were performed first and the Fru-2,6-P_2 produced was measured by a conventional enzyme coupled assay. The reaction mixture contained 20 mM Tris●HCl (pH 8.5), 0.5 mM $MgCl_2$, 0.1mM ATP, and 10-20µg PFKFB3. The reaction was initiated by adding 0.05mM Fru-6-P and incubation at 25 °C for 10 min, and the concentration of Fru-2,6-P_2 was determined every 5 min. Fru-2,6-P_2 was measured using the potato pyrophosphate-dependent 6-phosphofructokinase (PPi-PF1K) activation assay in which NADH consumption by glycolytic pathway was measured at 340nm using a microplate reader (Model 3550-UV, Bio- Rad), as described in elsewhere.

Cell Culture, Transient Transfection, and Oxidant Treatments.

HeLa cells were obtained from ATCC and cultured in DMEM containing 2 mM glutamine, 10% fetal calf serum (FCS), 100 U/ml penicillin and 100 µg/ml streptomycin (all from GIBCO-BRL). All cells were cultured in a humidified incubator at 37°C, 5% CO_2. Cells expressing PFKFB3 and its mutant were established by transfecting cells with pcDNA3.1/myc-HisA-PFKFB3 WT and mutant(s) using GeneJuice® transfection reagent (Novagen). Overexpression of PFKFB3 was confirmed by immunoblotting analysis. BCNU [N,N'-bis(2-chloroethyl)-N-nitrosourea] and H_2O_2 (hydrogen peroxide) were from Sigma and used as described in the text.

Detection of N-methylation and S-Glutathionylation of PFKFB3 in HeLa cells.

For detection of endogenous PFKFB3 glutathionylation and methylation, cells were treated with 10 µM proteasome inhibitor MG132 for 8 hrs. The whole cell lysates were prepared in a modified RIPA buffer (0.01 M sodium phosphate pH 7.2), 150 mM NaCl, 0.1mM EDTA, 1% Nonidet P-40, 1% sodium deoxycholate, and 0.1% SDS, 10 mM N-ethyl maleimide (NEM) supplemented with a protease inhibitor mixture (Roche) without reducing agent, to avoid changes in the S-glutathionylation status. Samples were immunoprecipitated using anti-PFKFB3 antibody, to enrich PFKFB3, and then resolved in non-reducing SDS-PAGE and subsequently transferred to nitrocellulose membranes.

Determination of Cellular Metabolites.

HeLa cells were plated at a density of $1x10^7$ in T 175 culture flasks in DMEM containing 10% FCS, 2 mM glutamine, 100 U/ml penicillin and 100 µg/ml streptomycin. After 36 hours of incubation, the media were replaced with fresh DMEM containing either H_2O_2, AdOX, or GSHee at the indicated concentrations and time.

Media samples were collected for measuring the lactate secretion levels using a lactate oxidase-based assay kit (Sigma-Aldrich). Cell extracts were prepared with the lysis buffer containing 0.01 M sodium phosphate (pH 7.5), 150 mM NaCl, 5 mM EDTA, 1% Nonidet P-40, and 5% 5-sulfosalicylic acid. Before each assay, ice cold 2M KOH was added to the SSA- preserved sample for neutralization. The Fru-2,6-P_2 level was determined in the collected cells after the treatment by the method described previously.

For the quantification of the PPP, levels of ribulose 5-phosphate (Ribul-5P) and xylulose-5-phosphate (Xyl-5P) were monitored [37,38,45]. For this, the mixture of Ribul-5P, Xyl-5P, and glyceraldehydes-3-phosphate (G-3P) was quantitated first and the quantity of G-3P was subtracted. First, the quantification of mixture of the three was performed in a system containing 58 mM glycylglycine, 3.3 mM Xyl-5P, 0.002% (w/v) cocarboxylase, 15 mM magnesium chloride, 0.14 mM ß-nicotinamide adenine dinucleotide, reduced form, 15 mM $MgCl_2$, 20 units a-glycerophosphate dehydrogenase, 5 units triosephosphate isomerase, 0.1 unit ribulose 5-phosphate 3-epimerase, and 5 units transketolase as described previously . Then, levels of G-3P have been measured under the same condition but in the absence of ribulose 5-phosphate 3-epimerase and transketolase. Protein concentration was measured using QuantiPro BCA assay kit (Sigma-Aldrich) and metabolite concentrations were normalized to the total cellular protein concentration.

NADPH/NADP and GSH/GSSG measurements

Cells were prepared as described above in *Metabolite determination*. The cellular NADP/NADPH ratios and GSH/GSSG ratios were analyzed spectrophotometrically by using a reGSH/oxGSH measurement kit or NADPH assay kit (Abcam) according to the manufacturer's instructions.

Results and Discussion:

Catalytic Fru-6-P binding and the Fru-6-P entrance turn

Structural characteristics involved in the catalytic binding of Fru-6-P to the 6-phosphofructo-2-kinase domain of PFKFB3 are shown in Figure 1. Positions of the structural elements important for Fru-2,6-P_2 synthesis are shown in Figure 1A. One PFKFB3 subunit from the functional homodimer is shown as a C_α tracing and the individual substrate pockets are indicated by the bound ATP and Fru-6-P revealed in the pseudo-Michaelis complex structure (pdb '2DWP') [35]. The β-strand crucially employed for the dimeric interface and the two helices, an α-helix (residues 130-145) and a π-helix (-^{202}Asp-Pro-Asp-Lys-Cys-Asp^{207}-), are labeled as 'Dimer', 'α-h', and 'π-h', respectively. The first turn of the α-helix that is a part of the Fru-6-P entrance to the catalytic pocket is marked with a yellow star to indicate its relative positions in the entire PFKFB3 molecule.

In Figure 1B, the Fru-6-P entrance α-helix turn (-^{130}Thr-Arg-Glu-Arg-Arg^{134}-) is shown with Arg131/134, which is the N-CH3 site, and Arg133, which is the Fru-6-P binding residue. Arg133 undergoes a ~4 Å down swing from its free enzyme position (gray, pdb '2AXN') to form a strong divalent salt bridge to the 6-phosphate moiety of bound Fru-6-P or Fru-2,6-P_2 (in pdb '2DWP' and '2I1V', respectively). As revealed long time ago in the study of PFKFB1, the liver-type PFKFB isoform, Arg131 and Arg134 have been considered important for attracting the negatively charged substrate, Fru-6-P, to the catalytic pocket [46]. Supporting the idea, the amino acid sequence of this turn is strictly conserved among all four PFKFB isoforms, whereas the rest of the helix is relatively varied (data not shown). Confirming the suggested role of Arg131, its mutagenesis to Ala (Arg131→Ala) nearly abolished the activity but over 50% the wild-type activity was retained, when the positive charge was conserved by Arg131→Lys mutagenesis, as shown in Figure 1C.

The structural features of PFKFB3 suggest that this Fru-6-P entrance turn undergoes a significant conformational change to accommodate Fru-6-P into the catalytic pocket [32,35]. However, the conformational change is limited by its coupling to the neighboring π-helix (-^{204}DKCDRD-) through dual hydrogen bonds between Arg131/134 and Asp207 in the π-helix (Figure 1B). This coupling is stably protected by core hydrophobic interactions between Leu210, Leu138, and Phe150. Consequently, the substrate binding and, thereby, the enzymatic activity is limited by this coupling. Supporting this rationale, when this coupling was removed by Asp207→Ala mutagenesis, a 5-fold increase in the activity, the specific activity (k_{cat}/K_m) more precisely, was observed. (Figure 1C and Table 1). Taken together, conformational flexibility of the Fru-6-P entrance (-^{130}Thr-Arg-Glu-Arg-Arg^{134}-) is an important molecular paradigm in controls of the PFKFB3 activity.

Confirming this paradigm, S-Gsh of PFKFB3 at Cys206 caused a 4-fold decrease in the PFKFB3 activity [32]. The crystal structure of S-glutathionylated PFKFB3 (pdb '4MA4') revealed that the glutathione moiety (GSH, Glu-Cys-Gly) attached to Cys206 causes a dual structure/function effect. A bulky negatively charged GSH moiety (green in Figure 1D) attached to nearby the catalytic pocket impedes charge-attracted Fru-6-P binding by neutralizing charges of the Arg residues, as Arg131→Ala mutagenesis does (Table 1). More importantly, the attached GSH restrains conformational change, which is required upon the Fru-6-P binding. As shown in Figure 1D, the attached GSH provides multiple hydrogen bonds to main chain N of Glu132, the side chain of Arg131, and helix-capping Gln198, decreasing the conformational flexibility of the Fru-6-P entrance. Taken together, the PFKFB3 activity is doubly compromised upon S-Gsh to cause the observed deactivation.

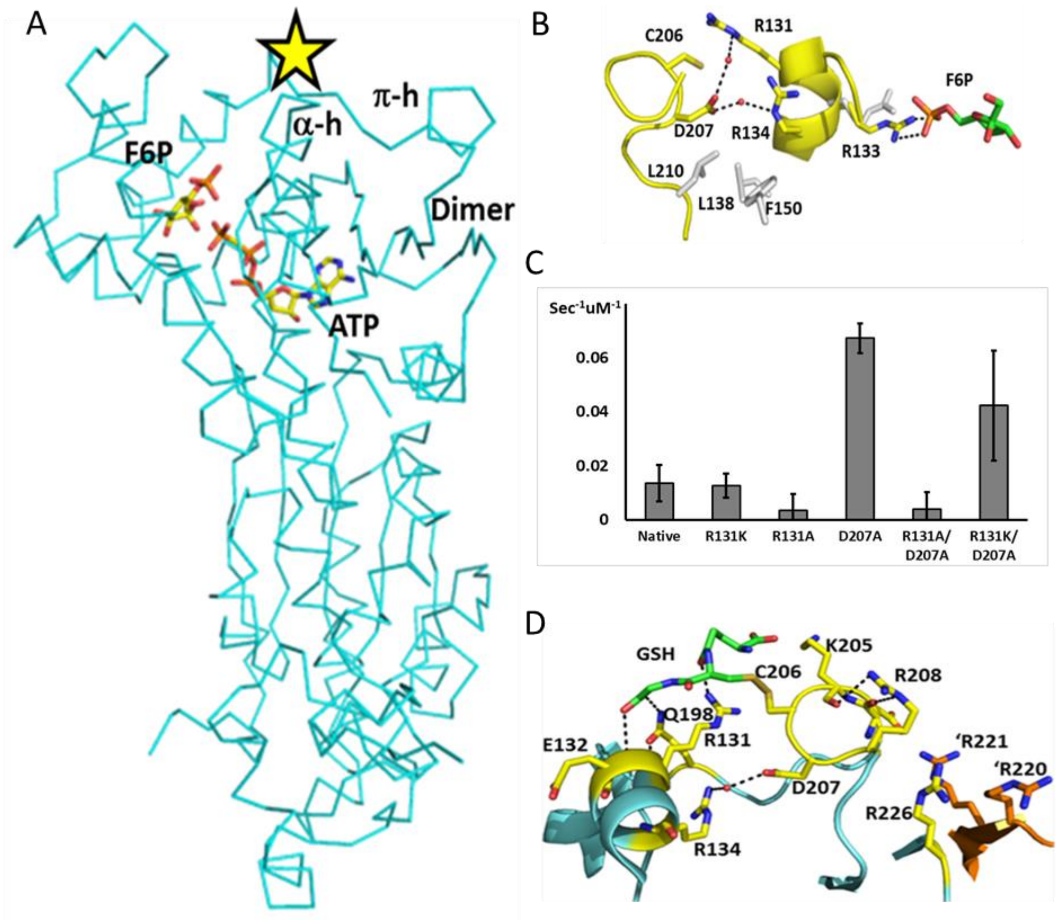

Figure 1. Structural paradigm of Fru-6-P binding and PFKFB3 activity. A. Structure of monomeric PFKFB3 (cyan). ATP and Fru-6-P bound to the catalytic pocket are shown colored sticks. The entrance of Fru-6-P to the catalytic pocket is marked with a yellow star. The helices neighboring the entrance and a strand employed in the dimeric interface are labeled accordingly: α-h, π-h, and Dimer, respectively. **B.** Role of the α-helix turn in Fru-6-P binding. Structural coupling between the α-helix (yellow ribbon) and the π-helix (yellow turn) by multivalent hydrogen bonds and the direct interaction between Fru-6-P and the turn

are shown as dotted lines. **C.** Effects of various site-directed mutagenesis on the PFKFB3 activity for Fru-2,6-P_2 production. The activities are represented relatively to the wild-type (Native). Mutagenesis is shown as R131K for Arg131→Lys for example. **D.** Structure of S-Glutathionylated PFKFB3. A glutathione moiety (green) attached to Cys206 in the π-helix (yellow turn) via a disulfide bond and its interactions with the α-helix is shown (Adopted from pdb'4MA4'). Residues from the dimeric interface strand are shown in orange.

Table 1. Kinetic properties of covalently modified or mutated PFKFB3

States	k_{cat} (sec^{-1})	K_m^{F6P} (μM)	K_m^{ATP} (μM)	k_{cat}/K_m^{F6P} ($sec^{-1}μM^{-1}$)
Native	0.15 ± 0.024	12.2 ± 2.8	16.7 ± 2.1	0.0136 ± 0.0067
S-Gsh	0.12 ± 0.032	49.5 ± 7.2	15.6 ± 3.4	0.0033 ± 0.0033
N-CH3	0.19 ± 0.074	2.8 ± 1.1	18.5 ± 4.4	0.0629 ± 0.0103
Asp207→A	0.20 ± 0.044	2.3 ± 0.7	17.3 ± 5.7	0.0673 ± 0.0056
Arg131→K	0.14 ± 0.037	53.6 ± 6.9	14.7 ± 2.9	0.0125 ± 0.0044
Arg131→A	0.16 ± 0.019	5.7 ± 1.6	16.2 ± 5.1	0.0035 ± 0.0061

Observations of these structure/function relationship altogether support that the conformational flexibility of the Fru-6-P entrance is an important control factor of PFKFB3 activity and, further, suggest that any molecular event that increases the conformational flexibility of this helix turn would increase the PFKFB3 activity. Tests of such a model became inevitable, because Arg131/134 of this F-6-P entrance turn was revealed to be asymmetrically di-methylated (N-CH3) by the actions of protein arginine methyl transferase 1 (PRMT1) inside cells. It is suspected that N-CH3 causes direct structural effects on the Fru-6-P entrance.

Structure/function effect of asymmetrical di-methylation at Arg131/134

Simulation: To have insights into the possible structural effect of N-CH3, the asymmetrical di-methylation at Arg131/134 were simulated using the energy minimization algorithm implemented in MOE under the Merck Molecular Force Field 94 [47,48]. For comparative structural analysis, the energy minimization was introduced onto both the native protein and the methylated protein and the resulting structures were superposed for analysis of differences. As shown in Figure 2A, the Fru-6-P entrance turn of the methylated PFKFB3 moves away from the π-helix by ~1.3 Å because of the four methyl groups crammed into a narrow space between the two helices. Di-methylated Arg131 moved away by ~3.5 Å from its native position to interact with Gln199 and Pro200 instead of Asp207. In comparison, Arg134 moved away by ~1.4 Å to enhance hydrophobic interactions between the added methyl groups and the protein hydrophobic core. As a result, the F-6-P entrance turn is uncoupled from the π-helix. The uncoupling was suspected to enhance conformational flexibility of the turn and, thereby, to facilitate the catalytic Fru-6-P binding.

Functional effect: For better understanding of the biological significance of N-CH3 of PFKFB3, its effect on the activity for Fru-2,6-P_2 production was investigated. The wild-type PFKFB3 and two site-directed mutants, Arg131→Lys and Arg131→Ala, were methylated *in-vitro*, to confirm the *in-vitro* site specificity of PRMT1. Western blot with anti-asymmetric dimethyl arginine antibody and its densitometric quantitative analysis showed that N-CH3 by PRMT-1 is specific for Arg131/134 (Figure 2B). The methylation level was decreased to 42% in the presence of 50 μM adenosine-2',3'- dialdehyde (AdOX), an accepted PRMT1 inhibitor, confirming the PRMT1 dependency [42,43,49]. The methylation levels of the two Arg131 mutants were also severely decreased to 23% and 15% in Arg131→Lys and Arg131→Ala, respectively, confirming that Arg131 is the major methylation site, as pointed out in [42]. The results altogether confirmed that Arg131 and Arg134 are the sites of PRMT1-dependent methylation (N-CH3) and showed that N-CH3 of PFKFB3 is reproducible *in-vitro*.

In Figure 2C, the functional effect of the *in-vitro* N-CH3 was compared to those of other known regulatory covalent modifications of PFKFB3, S-glutathionylation at Cys206 (S-Gsh) and phosphorylation at Ser461 (O-Pho). When compared to the untreated control (Native), O-Pho and S-Gsh caused a 4-fold increase and a 4-fold decrease in the activity, respectively, as reported previously (15,16,32,33). In comparison, N-CH3 caused a 5-fold increase in the activity and the magnitude was decreased to less than 50% in the presence of 50 μM AdOX, agreeing with the Western results. Taken together, the PFKFB3 activity for Fru-2,6-P_2 production is increased by PRMT1-dependent methylation at Arg131/134.

Structural effect: The structural model of activation from the simulation study was tested using the coupling-disabled Asp207→Ala site-directed mutant. As shown in Figure 2D, this mutant showed a 5-fold increase in the activity, mimicking the methylated PFKFB3. The observation suggests that N-CH3 and Asp207→Ala share mechanics for the enhancement of the activity. Supporting the notion, the activity of the Asp207→Ala mutant was not significantly further enhanced by N-CH3 and the Arg131→Ala mutant, either (D207A/CH3 and R131A/CH3, respectively, in Figure 2D). Taken together, N-CH3 at Arg131/134 facilitates the Fru-6-P binding by enhancing the conformational flexibility of the Fru-6-P entrance turn, to cause the observed activity enhancement. The idea was supported by the steady state kinetics summarized in Table 1. Both the activation by N-CH3 and Asp207→Ala caused near 5-fold decreases in the K_ms for Fru-6-P with no major changes in k_{cat}, whereas S-Gsh increased the K_m to a similar extent. It was also notable that ATP binding was not significantly affected by these covalent modifications or mutagenesis, confirming the simulation result.

Biological significance: To evaluate biological significance of the suggested N-CH3-dependent activity enhancement, the functional effect of N-CH3 on PFKFB3 inside cell was compared to that of the functionally opposing S-Gsh. HeLa cells were transformed to overexpress wild-type PFKFB3 (WT) in order to control the cellular PFKFB3 abundance and glycolytic rates (Figure 2E-G). The extent of N-CH3 was controlled by the treatment with 100 μM AdOX (AdOX) and S-Gsh was induced by 50 μM H_2O_2 (H_2O_2). To compare the effects of N-CH3 and S-Gsh of PFKFB3, the mutants, Arg131→A (R131A) and Cys206→A (C206A), were also expressed, the former as the control for low N-CH3 levels and the latter as that for low S-Gsh levels. Their effects on glycolysis and the pentose phosphate pathway (PPP) were characterized by assaying the Fru-2,6-P_2 levels and the NADPH levels.

As shown in the Western blots (Figure 2E), the PFKFB3 protein levels were increased by the overexpression. The N-CH3 level was kept as high as that of endogenous PFKFB3 (Endogenous) and the level was not affected by the employed vector (Vehicle). The N-CH3 level of R131A overexpressed was significantly lower than that of the wild-type but not notably higher than that of the endogenous. In comparison, the S-Gsh level of C206A was significantly lower than the wild-type but not notably lower than the endogenous. The Western blot results, thus, clearly show that Arg131 is the major site of N-CH3 and Cys206 of S-Gsh, as previously reported [32,42].

As expected, the overexpression of WT or C206A significantly increased the cellular Fru-2,6-P_2 levels to the similar extent, while R131A did not (Figure 2F, Native). That is because WT and C206A maintain high N-CH3 levels, whereas R131 does not. Supporting the rationale, when they were treated with AdOX to lower the N-CH3 levels, the magnitudes of increases were severely decreased (AdOX) and the decrease was maximal, when the oxidative stress (H2O2) was raised, resulting in a sharp decrease in the Fru-2,6-P_2 production. The decrease by oxidative stress was not shown in C206A, which is insensitive to S-Gsh.

Significant decreases in the Fru-2,6-P_2 levels causes a bottleneck in the glycolytic pathway at the step for conversion of Fru-6-P to Fru-1,6-P_2 and, as a result, the upstream substrates including Fru-6-P are rerouted into the PPP, resulting in increased production of NADPH (Figure 2G). The magnitude of this metabolic redirection and NADPH production were dependent on the abundance of PFKFB3 with the activity that can be decreased by the decreases in the N-CH3 levels (AdOX) or by the increases in the S-Gsh levels in a ROS-dependent manner (H2O2). Altogether, it was indicated that both N-CH3 and S-Gsh of PFKFB3 plays important role in the reciprocal activation of glycolysis and the PPP.

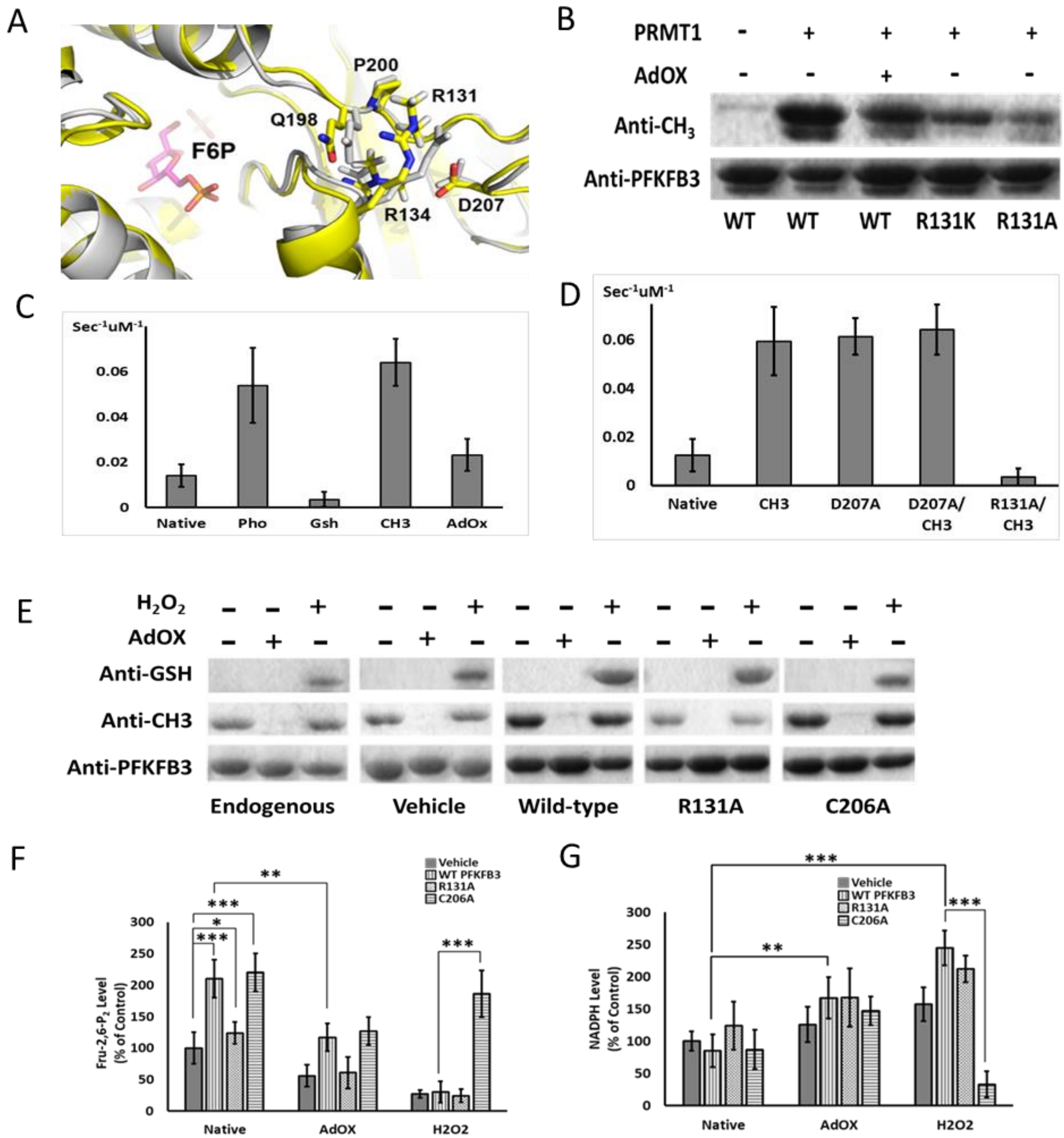

Figure 2. PRMT-1-dependent methylation of PFKFB3 at Arg131 and Arg134.
A. Computational prediction (MD) of structural changes in PFKFB3 by PRMT1-dependent asymmetrical di-methylation. The MD structure of the methylated protein (yellow) is superposed onto that of the native protein (gray). **B.** Immunoblots of purified recombinant PFKFB3 methylated by PRMT-1 and the effects of 100 μM AdOX, and site-directed mutagenesis on the methylation. **C.** Effects of various covalent modifications on the PFKFB3 activity. The activities of untreated (Native), phosphorylated by protein kinase A (Pho), S-glutathionylated (Gsh), methylated by PRMT-1 (CH3), and methylated by PRMT-1 in the presence of 50 μM AdOX (AdOX). **D.** Effects of various site-directed mutagenesis and the PRMT-1-dependent methylation on the PFKFB3 activity. **E.** Immunoblotting of various states of PFKFB3 in HeLa cells after the treatments for PFKFB3 modifications: untreated (Ctrl), 100 μM AdOX-treated for PRMT-1-

inhibition (AdOX), and 50 μM H_2O_2-treated for S-glutathionylation (H_2O_2). Endogenous, no treatment for protein over expression; Vehicle, empty vector transformed; Wild-type, the wild-type overexpressed; R131A, the Arg131→Ala mutant overexpressed; and C206A, the Cys206→Ala mutant overexpressed. **F.** The effect of diminished N-CH3 (AdOX) and S-Gsh (H2O2) on the cellular levels of Fru-2,6-P_2 and NADPH, when cells were treated the same as in the immunoblotting. Absolute values were normalized to the total protein concentration and changes in metabolite levels are expressed as a percent of control (Native, untreated). T-tests were performed against control (*, $P < 0.05$; **, $P < 0.01$; ***, $P < 0.001$; +, $P < 0.06$ (marginally significant); NS, not significant).

Relationship between N-CH3 and S-Gsh in PFKFB3 control

As described above, N-CH3 and S-Gsh are the covalent modifications that cause two functionally opposing effects. Interestingly, the two modifications occur to a nearly same area nearby the entrance to the catalytic pocket, as shown in Figure 1B. The distance between Arg131 for N-CH_3 and Cys206 for S-Gsh is only 3.7 Å, suggesting a possibility of interplay between the two opposing modifications. Considering that S-Gsh is a process carried out by a single tripeptide molecule, glutathione (GSH), S-Gsh is not likely to be impeded, whether the methyl groups are attached to Arg131/134 or not. On the other hand, N-CH3, an enzyme-catalyzed process, would be severely interfered, if Cys206 is attached with a GSH molecule in advance, because of its severe steric hindrance to the access of the enzyme, PRMT1.

This speculation was tested by investigating how one modification affects the other in terms of its efficacy and ultimate functional effects, using purified recombinant PFKFB3. As shown in Figure 3A, PFKFB3 methylated in advance could be additionally S-glutathionylated, when the oxidative stress levels were elevated by addition of 3 mM oxGSH (CH_3/Gsh). More surprisingly, as shown in Figure 3B, this additional S-Gsh (CH3/Gsh) not only abolishes the activation by N-CH3 but also deactivates the enzyme, as if there was no previous N-CH3 at all in the protein. In other words, the deactivation by S-Gsh dominates in the functional effect on the PFKFB3 activity, whether S-Gsh is first or second, as shown as Gsh and CH3/Gsh, respectively. The functional effect of the additional S-Gsh on the methylated PFKFB3 is not different from that of S-Gsh on the native protein.

However, when S-Gsh was introduced in advance, the subsequent N-CH3 was negligible (Gsh/CH3 in Figure 3A) and the no changes in activity was accompanied (Gsh/CH3 in Figure 3B). The functional prevalence of S-Gsh in the methylated protein is attributable to the interactions of the GSH moiety with the Fru-6-P turn residues as described above and shown in Figure 1D. It is likely that, although N-CH3 uncouples the turn from the π-helix, the GSH attached to Cys206 freeze the conformation of the turn its increased interactions to the turn and neighboring structures.

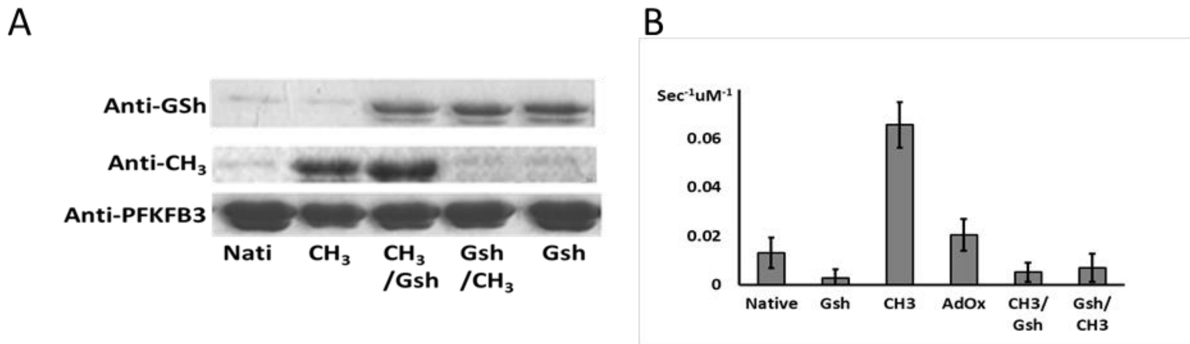

Figure 3. Interplay of PRMT-1-dependent asymmetrical di-methylation and S-glutathionylation in PFKFB3. A. Immunoblotting of PFKFB3 after the dual modifications: untreated (Nati), PRMT-1-dependent N-methylation (CH3), S-glutathionylation (Gsh), S-glutathionylation after N-methylation (CH3/Gsh), N-methylation after S-glutathionylation (Gsh/CH3). **B.** Effects of the dual modifications on the PFKFB3 activity: untreated (Native), S-glutathionylation (Gsh), PRMT-1-dependent N-methylation (CH3), 100 µM AdOX (AdOX), S-glutathionylation after N-methylation (CH3/Gsh), N-methylation after S-glutathionylation (Gsh/CH3).

These results altogether suggest that the deactivation effect of S-Gsh on PFKFB3 would be prevalent, whenever the oxidative stress level is elevated. Onsets of excessive oxidative stress would induce S-Gsh of PFKFB3 even though most PFKFB3 exist as the methylated form inside cell. As a consequence, the cellular Fru-2,6-P_2 levels would be promptly decreased and, thereby, the glycolytic flux would be redirected to the pentose phosphate pathway (PPP) for enhanced production of NADPH for neutralization of reactive oxygen species (ROS) [32,37,38]. Thus, it can be projected that a mechanism crucial for cell survival from oxidative stress would overrule a mechanism for steady cell growth, when endangered by oxidative stress.

Interplay between S-Gsh and N-CH3 for PFKFB3 control inside cell

The interplay between S-Gsh and N-CH3 for the control of PFKFB3 inside cell was investigated. HeLa cells were transformed to overexpress PFKFB3, cultured, and treated in a way to change the modification states of cellular PFKFB3 and the results were analyzed using Western blots of cell extracts (Figure 4A). The cells were untreated to maintain a higher level of N-CH3 (Control); and/or a treated with 100 µM AdOX, PRMT1 inhibitor, to decrease the N-CH_3 level (AdOX); and/or 50 µM H_2O_2 to induce S-Gsh of PFKFB3 (H2O2). To test the effect of preexisting N-CH3 on the additional S-Gsh, S-Gsh of PFKFB3 with a higher level of the previous N-CH3 (H2O2) and that with a lower level of N-CH3 (AdOX + H2O2) were compared. To test the effect of preexisting S-Gsh on the additional N-CH3, the (AdOX + H2O2) cells were transferred to the medium with no AdOX to allow restoration of N-CH3 (AdOX + H2O2 – AdOX).

Consistently with the results from the recombinant protein experiments, a near abolishment of N-CH3 was caused by the treatment with excessive 100 µM AdOX (AdOX), compared to the untreated control (Control). However, when cellular oxidative stress level was elevated by the H_2O_2 treatment, not only native PFKFB3 but also PFKFB3 methylated in advance was S-glutathionylated (H2O2 and AdOX+H2O2, respectively), showing that S-Gsh is not affected by the previous N-CH3 as in the recombinant protein experiment described above and in Figure 3A. On the contrary, once S-glutathionylated, PFKFB3 was no longer subject to N-CH3 (AdOX+H_2O_2-AdOX). Taken together, elevated oxidative stress can cause S-glutathionylation of PFKFB3, whether it is previously methylated or not.

Furthermore, it was observed that PFKFB3 control by S-Gsh and N-CH3 was followed by the metabolic effects. Changes in glycolytic flux were characterized by changes in Fru-2,6-P_2 levels (Figure 4B) and secreted lactate levels (Figure 4C), while those in the PPP were by Ribulose-5-phosphate + Xylulose-5-P concentration levels (Figure 4D), NADPH/NADP concentration ratios (Figure 4E), and reduced/oxidized glutathione (reGSH/oxGSH) concentration ratios (Figure 4F). As shown in Figure 4B and 4C, decreases in N-CH3 levels by the AdOX treatment were reflected in decreases in the levels of Fru-2,6-P_2 and secreted lactate to a similar extent, supporting the speculation that N-CH3 is a mechanism for activation of PFKFB3 and glycolysis. However, when cellular oxidative stress was elevated by the H_2O_2 treatment, S-Gsh of PFKFB3 was increased. As shown in Figure 4D-F, all the tested PPP metabolites and reGSH were increased after the H_2O_2 treatment, reflecting the covalent modification effects shown in Figure 4A.

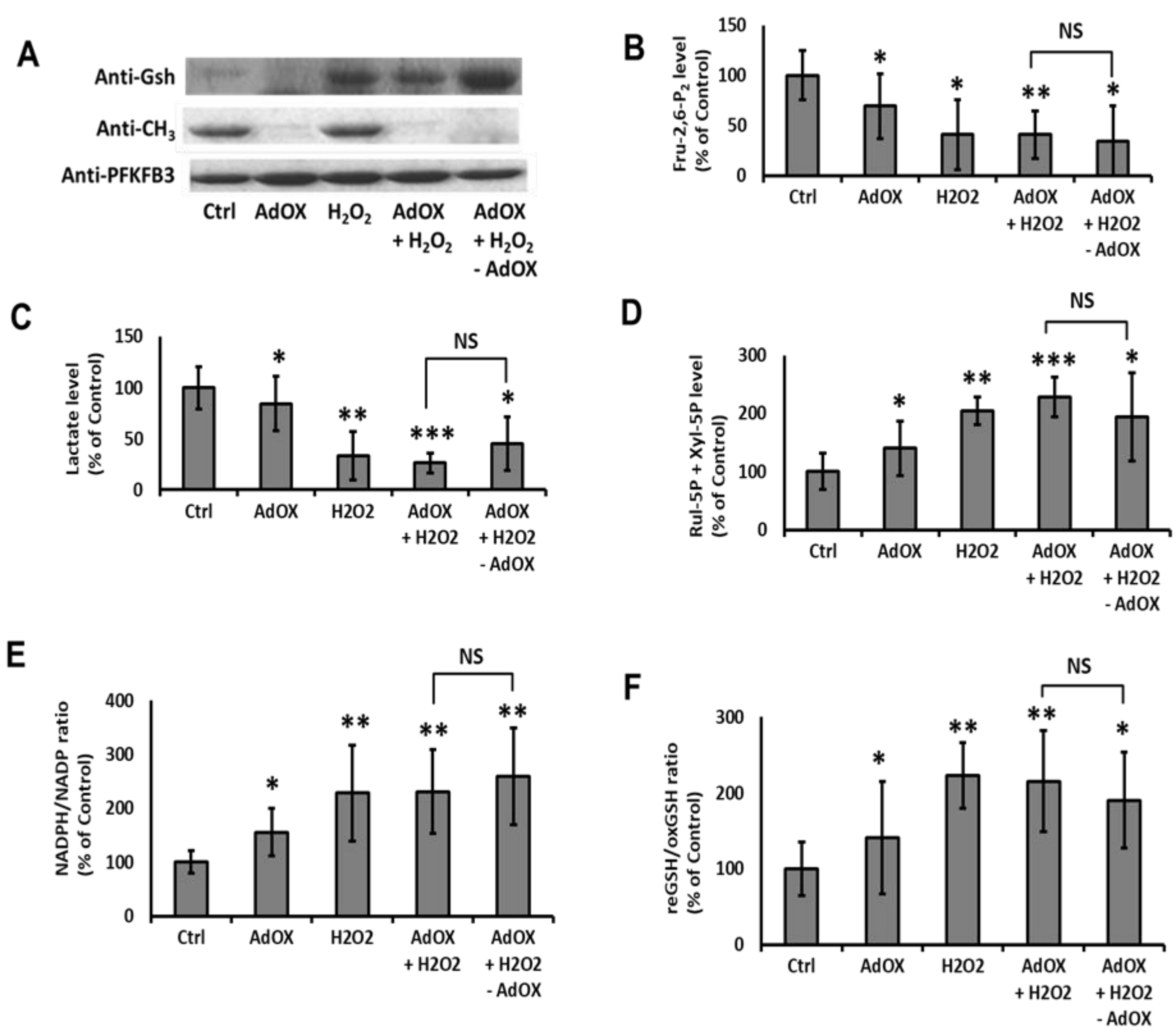

Figure 4. Effects of the dual modifications on PFKFB3 and metabolism inside HeLa cells. A. Immunoblotting of PFKFB3 overexpressed in HeLa cells after the treatments for PFKFB3 modifications: untreated (Ctrl), 50 μM AdOX-treated for PRMT-1-inhibition (AdOX), 50 μM H_2O_2-treated for S-glutathionylation (H_2O_2), treated with 50 μM H_2O_2 after with 50 μM AdOX (AdOX+ H_2O_2), washed with medium with no AdOX to remove AdOX but not H_2O_2 (AdOx+ H_2O_2-AdOX). **B.-F.** Effects on Fru-2,6-P_2 levels (**B**), secreted lactate levels (**C**), Ribulose-5-phosphate/Xylulose-5-P levels (**D**), NADPH/NADP ratios (**E**), and GSH/GSSG ratios (**F**), when cells were treated the same as in the immunoblotting. Absolute values were normalized to the total protein concentration and changes in metabolite levels are expressed as a percent of control. T-tests were performed against control (*, $P < 0.05$; **, $P < 0.01$; ***, $P < 0.001$; +, $P < 0.06$ (marginally significant); NS, not significant). Additional T-tests were performed between the groups of AdOX+H2O2 and AdOX+H2O2-AdOX.

Taken together, modulation of PFKFB3 activity by the H_2O_2 treatment decreased glycolysis and increased the PPP, resulting in an increase in NADPH/NADP ratio and, ultimately, an increase in reGSH/oxGSH ratios. An increase in PPP flux and, thereby, reGSH/oxGSH concentration ratios is crucial for regulating cellular ROS levels and, ultimately, cell survival under oxidative stress. Thus, our results reconfirm that S-Gsh of PFKFB3 controls glucose metabolism for regulation of oxidative stress homeostasis.

Biological significance

The results altogether reveal that the PFKFB3 activity is controlled by N-CH3 and S-Gsh, which occur to the same protein area but for the practically opposing functional effects. The relationship between the two covalent controls of PFKFB3 is analogous to the 'Yin-Yang' relationship between phosphorylation (O-Pho) and O-linked glycosylation with N-acetylglucosamine (O-GlcNAc) in dual covalent controls adopted in many other proteins [50-52]. As well documented, O-Pho and O-GlcNAc compete for the same or nearby serine/threonine residues such that the one exerts exclusive influence on the other by exerting steric hindrance to both the protein-dependent modifications [51,53].

However, N-CH3 and S-Gsh in PFKFB3 is uniquely different from the typical 'Yin-Yang' relationship. Because S-Gsh is accomplished by a protein-free process, which is insensitive to prior N-CH3, N-CH3 and S-Gsh unevenly compete for the same area of PFKFB3. Moreover, the S-Gsh effect is released only after oxidative stress was subdued by activation of the PPP and the resulting increases in reGSH. This uneven relationship between the two control mechanisms would force continuous cycles of glycolysis and the PPP for regulation of cellular oxidative stress homeostasis, as diagramed in Figure 5.

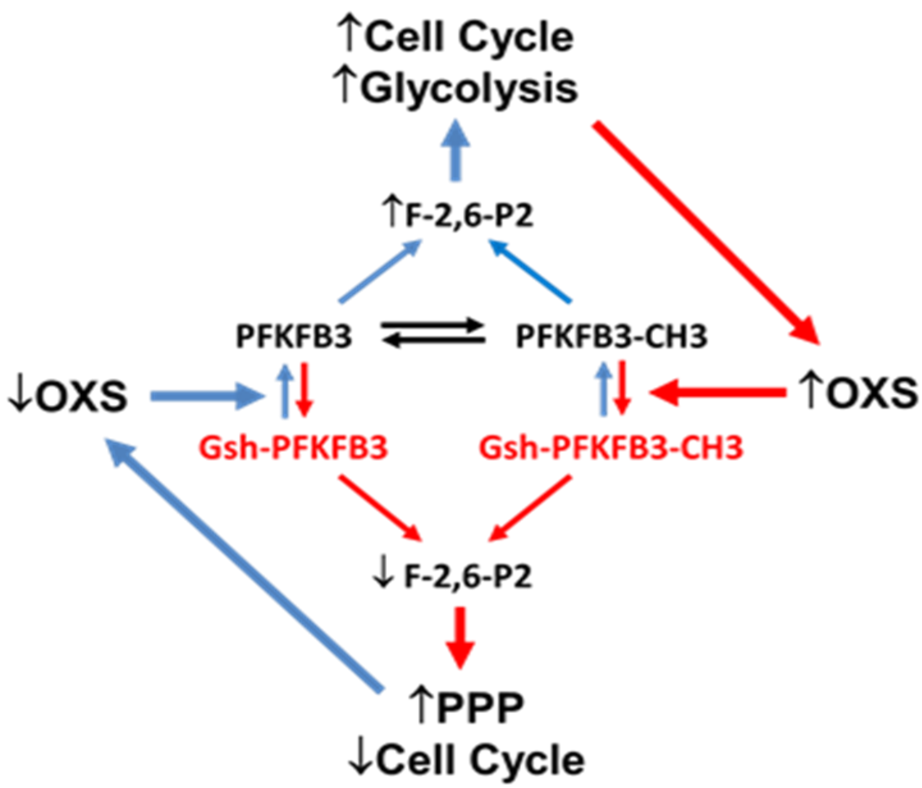

Figure 5. Cyclic activation of glucose metabolisms by covalent control of PFKFB3. The uneven competitive relationship between N-CH3 and S-Gsh force continuous cycles of glycolysis and the PPP for regulation of cellular oxidative stress homeostasis. To avoid the detrimental oxidative stress (OXS), which is easily induced by activated glycolysis in tumor cells (Red), up-regulation of NADPH and, thereby, reGSH, via the PPP (Blue) is necessary for detoxification of ROS. To achieve alternative activation of glycolysis and the PPP, the PFKFB3 activity for production of Fru-2,6-P_2 is crucially controlled by cellular oxidative stress via S-Gsh. PFKFB3-CH3, N-methylated PFKFB3; Gsh-PFKFB3, S-glutathionylated PFKFB3; Gsh-PFKFB3-CH3, PFKFB3 both N-methylated and G-glutathionylated; and OXS, oxidative stress.

Activation of aerobic glycolysis and mitochondrial impairment is the two hallmarks of tumor cells and, as a result of such metabolic reprogramming, cellular oxidative stress easily increases to detrimental levels. To avoid the detrimental conditions, up-regulation of the PPP and, thereby, reGSH, which is recycled using NADPH produced from the PPP, is necessary for detoxification of ROS. In that regard, it is interesting that the PFKFB3 activity for production of Fru-2,6-P_2, which is the key allosteric regulator of glycolysis, is crucially controlled by cellular oxidative stress via S-Gsh, because decreases in cellular Fru-2,6-P_2 levels and glycolysis is coupled to a reciprocal increase in the PPP. It is even more interesting to find that S-Gsh, a survival mechanism, can overrule N-CH3, a growth mechanism, to ensure the metabolic shifts crucially required for coping with onsets of detrimental oxidative stress.

Periodical alternative activation of glycolysis and the PPP is also necessary for biosynthesis of nucleotides, some amino acids, and lipids for rapid cell proliferation in cancer [2,34,37]. Activation of glycolysis is not only for energy production but also for production of the glycolytic intermediate metabolites used as precursors of the anabolic processes. Modulation of PFKFB3 enables cells to secure large quantities of the glycolytic metabolites necessary for such anabolic processes. Otherwise, a harmonious biosynthesis using the PPP products would not be possible. In this regard, PFKFB3 control by S-Gsh also suggests a possible role of PFKFB3 in cell cycle progression of cancer cells, although further studies are necessary to

Continued cell cycle progression of proliferation of tumor requires metabolic alteration of cellular glucose to glycolysis and the PPP for production of energy and materials. It has been shown that the alternation is achieved by dynamic covalent modifications of PFKFB3 and the resulting changes in the level of Fru-2,6-P_2. We have shown that N-CH3 at Arg131/134 is for up-regulation of Fru-2,6-P_2, while S-Gsh at Cys206 for down-regulation. Moreover, the two functionally opposing mechanisms controls the PFKFB3 activity in a cyclic manner such that tumor cells steadily continue cell division, avoiding detrimental effects of ever-increasing ROS.

elucidate the details of this mechanism. This new understanding will contribute to the development of appropriate therapeutic strategies for cancer prevention and treatment based on their redox profile.

Conclusion

Acknowledgments: Funding for this study was partly provided by grants to Y.-H.L from the National Cancer Institute (1R01 CA124758-01). We would like to thank Theresa Lee for critical reading of the manuscript.

Author Contributions: J.K. designed and performed cloning, protein experiments, and cell study; Y.Y. prepared protein and performed enzyme assay; M.B. performed MD; R.M. performed cloning and cell study; and Y.L. supervised and directed the project and wrote the manuscript.

References:

1. Chesney J, Mitchell R, Benigni F, et al. An inducible gene product for 6-phosphofructo-2-kinase with an AU-rich instability element: role in tumor cell glycolysis and the Warburg effect. *Proc Natl Acad Sci U S A*. Mar 16 1999;96(6):3047-52.
2. Franklin DA, He Y, Leslie PL, et al. p53 coordinates DNA repair with nucleotide synthesis by suppressing PFKFB3 expression and promoting the pentose phosphate pathway. *Sci Rep*. Nov 30 2016;6:38067. doi:10.1038/srep38067
3. Branco C, Johnson RS. To PFKFB3 or Not to PFKFB3, That Is the Question. *Cancer Cell*. Dec 12 2016;30(6):831. doi:10.1016/j.ccell.2016.11.007
4. Ge X, Lyu P, Cao Z, et al. Overexpression of miR-206 suppresses glycolysis, proliferation and migration in breast cancer cells via PFKFB3 targeting. *Biochem Biophys Res Commun*. Aug 07 2015;463(4):1115-21. doi:10.1016/j.bbrc.2015.06.068
5. Calvo MN, Bartrons R, Castano E, Perales JC, Navarro-Sabate A, Manzano A. PFKFB3 gene silencing decreases glycolysis, induces cell-cycle delay and inhibits anchorage-independent growth in HeLa cells. *FEBS Lett*. May 29 2006;580(13):3308-14. doi:10.1016/j.febslet.2006.04.093
6. Atsumi T, Nishio T, Niwa H, et al. Expression of inducible 6-phosphofructo-2-kinase/fructose-2,6-bisphosphatase/PFKFB3 isoforms in adipocytes and their potential role in glycolytic regulation. *Diabetes*. Dec 2005;54(12):3349-57.
7. Minchenko A, Leshchinsky I, Opentanova I, et al. Hypoxia-inducible factor-1-mediated expression of the 6-phosphofructo-2-kinase/fructose-2,6-bisphosphatase-3 (PFKFB3) gene. Its possible role in the Warburg effect. *J Biol Chem*. Feb 22 2002;277(8):6183-7.
8. Atsumi T, Chesney J, Metz C, et al. High expression of inducible 6-phosphofructo-2-kinase/fructose-2,6-bisphosphatase (iPFK-2; PFKFB3) in human cancers. *Cancer Res*. Oct 15 2002;62(20):5881-7.
9. Depre C, Veitch K, Hue L. Role of fructose 2,6-bisphosphate in the control of glycolysis. Stimulation of glycogen synthesis by lactate in the isolated working rat heart. *Acta Cardiol*. 1993;48(1):147-64.
10. Pilkis SJ, Granner, D.K. . Molecular physiology of the regulation of hepatic gluconeogenesis and glycolysis. *Ann Rev Physiol*. 1992;54:885-909.
11. Ogush S, Lawson JW, Dobson GP, Veech RL, Uyeda K. A new transient activator of phosphofructokinase during initiation of rapid glycolysis in brain. *J Biol Chem*. Jul 5 1990;265(19):10943-9.
12. Pilkis SJ, El-Maghrabi MR, Claus TH. Hormonal regulation of hepatic gluconeogenesis and glycolysis. . *Ann Rev Biochem*. 1988;55:755-783.
13. Rousseau GG, Hue L. Mammalian 6-phosphofructo-2-kinase/ fructose-2,6-bisphosphatase: a bifunctional enzyme that controls glycolysis. . *Prog Nucl Acid Res Mol Biol*. 1993;45:99-127.
14. Pilkis SJ, Claus TH, Kurland IJ, Lange AJ. 6-phosphofructo-2-kinase/ fructose-2,6-bisphosphatase: A metabolic signaling enzyme. *Annu Rev Biochem*. 1995;64:799-835.
15. El-Maghrabi MR, Noto F, Wu N, Manes N. 6-phosphofructo-2-kinase/fructose-2,6-bisphosphatase: suiting structure to need, in a family of tissue-specific enzymes. *Curr Opin Clin Nutr Metab Care*. Sep 2001;4(5):411-8.
16. Yalcin A, Clem BF, Imbert-Fernandez Y, et al. 6-Phosphofructo-2-kinase (PFKFB3) promotes cell cycle progression and suppresses apoptosis via Cdk1-mediated phosphorylation of p27. *Cell Death Dis*. 2014;5:e1337. doi:10.1038/cddis.2014.292
17. Verbon EH, Post JA, Boonstra J. The influence of reactive oxygen species on cell

cycle progression in mammalian cells. Review. *Gene*. Dec 10 2012;511(1):1-6. doi:10.1016/j.gene.2012.08.038
18. Boonstra J, Post JA. Molecular events associated with reactive oxygen species and cell cycle progression in mammalian cells. Review. *Gene*. Aug 4 2004;337:1-13. doi:10.1016/j.gene.2004.04.032
19. Perez JX, Roig T, Manzano A, et al. Over expression of fructose-2,6-bisphosphatase decreases glycolysis and cell cycle progression. *Am J Physiol Cell Physiol*. 2000;279:C1359-C1364.
20. Cantelmo AR, Conradi LC, Brajic A, et al. Inhibition of the Glycolytic Activator PFKFB3 in Endothelium Induces Tumor Vessel Normalization, Impairs Metastasis, and Improves Chemotherapy. *Cancer Cell*. Dec 12 2016;30(6):968-985. doi:10.1016/j.ccell.2016.10.006
21. De Bock K, Georgiadou M, Schoors S, et al. Role of PFKFB3-driven glycolysis in vessel sprouting. *Cell*. Aug 1 2013;154(3):651-63. doi:10.1016/j.cell.2013.06.037
22. Garber K. Energy boost: the Warburg effect returns in a new theory of cancer. *J Natl Cancer Inst*. Dec 15 2004;96(24):1805-6.
23. Zhu W, Ye L, Zhang J, et al. PFK15, a Small Molecule Inhibitor of PFKFB3, Induces Cell Cycle Arrest, Apoptosis and Inhibits Invasion in Gastric Cancer. *PLoS One*. 2016;11(9):e0163768. doi:10.1371/journal.pone.0163768
24. Xu Y, An X, Guo X, et al. Endothelial PFKFB3 plays a critical role in angiogenesis. *Arterioscler Thromb Vasc Biol*. Jun 2014;34(6):1231-9. doi:10.1161/ATVBAHA.113.303041
25. Boyd S, Brookfield JL, Critchlow SE, et al. Structure-Based Design of Potent and Selective Inhibitors of the Metabolic Kinase PFKFB3. *J Med Chem*. Apr 23 2015;58(8):3611-25. doi:10.1021/acs.jmedchem.5b00352
26. Clem BF, O'Neal J, Tapolsky G, et al. Targeting 6-phosphofructo-2-kinase (PFKFB3) as a therapeutic strategy against cancer. *Mol Cancer Ther*. Aug 2013;12(8):1461-70. doi:10.1158/1535-7163.MCT-13-0097
27. Seo M, Kim JD, Neau D, Sehgal I, Lee YH. Structure-based development of small molecule PFKFB3 inhibitors: a framework for potential cancer therapeutic agents targeting the Warburg effect. *PLoS One*. 2011;6(9):e24179. doi:10.1371/journal.pone.0024179
28. Crochet RB, Cavalier MC, Seo M, et al. Investigating combinatorial approaches in virtual screening on human inducible 6-phosphofructo-2-kinase/fructose-2,6-bisphosphatase (PFKFB3): a case study for small molecule kinases. *Analytical biochemistry*. Nov 1 2011;418(1):143-8. doi:10.1016/j.ab.2011.06.035
29. Reid MA, Lowman XH, Pan M, et al. IKKbeta promotes metabolic adaptation to glutamine deprivation via phosphorylation and inhibition of PFKFB3. *Genes Dev*. Aug 15 2016;30(16):1837-51. doi:10.1101/gad.287235.116
30. Bando H, Atsumi T, Nishio T, et al. Phosphorylation of the 6-phosphofructo-2-kinase/fructose 2,6-bisphosphatase/PFKFB3 family of glycolytic regulators in human cancer. Comparative Study. *Clinical cancer research*. Aug 15 2005;11(16):5784-92. doi:10.1158/1078-0432.CCR-05-0149
31. Rider MH, Bertrand L, Vertommen D, Michels PA, Rousseau GG, Hue L. 6-phosphofructo-2-kinase/fructose-2,6-bisphosphatase: head-to-head with a bifunctional enzyme that controls glycolysis. *Biochem J*. Aug 1 2004;381(Pt 3):561-79.
32. Seo M, Lee YH. PFKFB3 regulates oxidative stress homeostasis via its S-glutathionylation in cancer. *J Mol Biol*. Feb 20 2014;426(4):830-42. doi:10.1016/j.jmb.2013.11.021

33. Tudzarova S, Colombo SL, Stoeber K, Carcamo S, Williams GH, Moncada S. Two ubiquitin ligases, APC/C-Cdh1 and SKP1-CUL1-F (SCF)-beta-TrCP, sequentially regulate glycolysis during the cell cycle. Research Support, Non-U.S. Gov't. *Proceedings of the National Academy of Sciences of the United States of America*. Mar 29 2011;108(13):5278-83. doi:10.1073/pnas.1102247108
34. Vizan P, Alcarraz-Vizan G, Diaz-Moralli S, Solovjeva ON, Frederiks WM, Cascante M. Modulation of pentose phosphate pathway during cell cycle progression in human colon adenocarcinoma cell line HT29. Research Support, Non-U.S. Gov't. *International journal of cancer Journal international du cancer*. Jun 15 2009;124(12):2789-96. doi:10.1002/ijc.24262
35. Kim SG, Cavalier M, El-Maghrabi MR, Lee YH. A direct substrate-substrate interaction found in the kinase domain of the bifunctional enzyme, 6-phosphofructo-2-kinase/fructose-2,6-bisphosphatase. Research Support, Non-U.S. Gov't. *Journal of molecular biology*. Jun 29 2007;370(1):14-26. doi:10.1016/j.jmb.2007.03.038
36. Kim SG, Manes NP, El-Maghrabi MR, Lee YH. Crystal structure of the hypoxia-inducible form of 6-phosphofructo-2-kinase/fructose-2,6-bisphosphatase (PFKFB3): a possible new target for cancer therapy. Research Support, Non-U.S. Gov't. *The Journal of biological chemistry*. Feb 3 2006;281(5):2939-44. doi:10.1074/jbc.M511019200
37. Boada J, Roig T, Perez X, et al. Cells overexpressing fructose-2,6-bisphosphatase showed enhanced pentose phosphate pathway flux and resistance to oxidative stress. Research Support, Non-U.S. Gov't. *FEBS letters*. Sep 1 2000;480(2-3):261-4.
38. Urner F, Sakkas D. Characterization of glycolysis and pentose phosphate pathway activity during sperm entry into the mouse oocyte. Research Support, Non-U.S. Gov't. *Biology of reproduction*. Apr 1999;60(4):973-8.
39. Israelsen WJ, Dayton TL, Davidson SM, et al. PKM2 Isoform-Specific Deletion Reveals a Differential Requirement for Pyruvate Kinase in Tumor Cells. *Cell*. Oct 10 2013;155(2):397-409. doi:10.1016/j.cell.2013.09.025
40. Anastasiou D, Poulogiannis G, Asara JM, et al. Inhibition of pyruvate kinase M2 by reactive oxygen species contributes to cellular antioxidant responses. *Science*. Dec 2 2011;334(6060):1278-83. doi:10.1126/science.1211485
41. Yi W, Clark PM, Mason DE, et al. Phosphofructokinase 1 glycosylation regulates cell growth and metabolism. *Science*. Aug 24 2012;337(6097):975-80. doi:10.1126/science.1222278
42. Yamamoto T, Takano N, Ishiwata K, et al. Reduced methylation of PFKFB3 in cancer cells shunts glucose towards the pentose phosphate pathway. *Nat Commun*. Mar 17 2014;5:3480. doi:10.1038/ncomms4480
43. Morales Y, Nitzel DV, Price OM, et al. Redox Control of Protein Arginine Methyltransferase 1 (PRMT1) Activity. *J Biol Chem*. Jun 12 2015;290(24):14915-26. doi:10.1074/jbc.M115.651380
44. Lee YH, Li Y, Uyeda K, Hasemann CA. Tissue-specific structure/function differentiation of the liver isoform of 6-phosphofructo-2-kinase/fructose-2,6-bisphosphatase. *J Biol Chem*. Jan 3 2003;278(1):523-30.
45. Moritz B, Striegel K, de Graaf AA, Sahm H. Changes of Pentose Phosphate Pathway Flux in Vivo in Corynebacterium glutamicum during Leucine-Limited Batch Cultivation as Determined from Intracellular Metabolite Concentration Measurements. *Metabolic Engineering*. 2002;4(4):295-305. doi:10.1006/mben.2002.0233
46. Bertrand L, Vertommen D, Depiereux E, Hue L, Rider MH, Feytmans E. Modelling

the 2-kinase domain of 6-phosphofructo-2-kinase/fructose-2,6-bisphosphatase on adenylate kinase. *Biochem J*. Feb 1 1997;321 (Pt 3):615-21.

47. Adams PD, Afonine PV, Bunkoczi G, et al. The Phenix software for automated determination of macromolecular structures. *Methods*. Sep 2011;55(1):94-106. doi:10.1016/j.ymeth.2011.07.005

48. TA H. Merck molecular force field. I. Basis, form, scope, parameterization, and performance of MMFF94. . *J Comput Chem*. 1996 17:490-519.

49. Yang Y, Bedford MT. Protein arginine methyltransferases and cancer. *Nat Rev Cancer*. Jan 2013;13(1):37-50. doi:10.1038/nrc3409

50. Ferron M, Denis M, Persello A, Rathagirishnan R, Lauzier B. Protein O-GlcNAcylation in Cardiac Pathologies: Past, Present, Future. *Front Endocrinol (Lausanne)*. 2018;9:819. doi:10.3389/fendo.2018.00819

51. Chen YX, Du JT, Zhou LX, et al. Alternative O-GlcNAcylation/O-phosphorylation of Ser16 induce different conformational disturbances to the N terminus of murine estrogen receptor beta. Research Support, Non-U.S. Gov't. *Chemistry & biology*. Sep 2006;13(9):937-44. doi:10.1016/j.chembiol.2006.06.017

52. Gloster TM, Vocadlo DJ. Mechanism, Structure, and Inhibition of O-GlcNAc Processing Enzymes. *Current signal transduction therapy*. Jan 2010;5(1):74-91.

53. Copeland RJ, Han G, Hart GW. O-GlcNAcomics-Revealing roles of O-GlcNAcylation in disease mechanisms and development of potential diagnostics. *Proteomics Clinical applications*. May 3 2013;doi:10.1002/prca.201300001

